Coarse-Fine Residual Gravity Cancellation System with Magnetic Levitation

S.E. Salcudean
Department of Electrical Engineering, University of British Columbia
2356 Main Mall, Vancouver, B.C., Canada, V6T 1W5

H. Davis, C.T. Chen, D.E. Goertz
Department of Physics, University of British Columbia
6224 Agricultural Road, Vancouver, B.C., Canada, V6T 1Z1

B.V. Tryggvason
Canadian Astronaut Program, Canadian Space Agency
Rockliffe Base, Ottawa, Ont., Canada, K1A 1A1

Abstract

Aircraft flights along parabolic trajectories have been proposed and executed in order to achieve low-cost, near free-fall conditions of moderate duration (*e.g.* NASA KC-135 flights). This paper describes a six degrees-of-freedom experiment isolation system designed to cancel out residual accelerations due to mechanical vibrations and errors in aircraft trajectory. The isolation system consists of a fine-motion magnetic levitator whose stator is transported by a conventional coarse-motion stage. The levitator uses wide-gap voice-coil actuators and has the dual purpose of isolating the experiment platform from aircraft vibrations and actively cancelling residual accelerations through feedback control. The coarse-motion stage tracks the levitated platform in order to keep the levitator's coils centered within their matching magnetic gaps. Aspects of system design, an analysis of the proposed control strategy and simulation results are presented. Feasibility experiments are also discussed.

I. Introduction

A number of scientific experiments require zero-gravity conditions. As an alternative to outer-space experiments and drop-towers, aircraft flights along parabolic trajectories have been proposed and executed in order to achieve low-cost, near free-fall conditions of moderate duration. Due to the deviation of the aircraft flight trajectory from a perfect parabola and due to mechanical vibrations, equipment that is solidly attached to the aircraft is still subject to small, unwanted, forces. At low frequencies, these forces are due to deviations in aircraft trajectory, while at high frequencies, these forces are due mainly to mechanical vibrations.
In order to deal with the problem of residual forces, large motion isolation mounts (LMIMs) have been proposed in joint studies between the Engineering Physics Department at the University of British Columbia (UBC) and the Canadian Astronaut Program [1, 2, 3]. The proposed approaches would allow low-friction, 3 DOF motion of an experimental setup (on an $x - y$ gantry with additional z motion) within a specified, encaged volume within the aircraft. Low-friction motion of the experimental platform with respect to the aircraft frame can be achieved by using air or magnetic bearings along each degree of freedom, thus isolating the experimental platform from the body of the aircraft. Such a large motion isolation mount would enable a closer approximation to free-fall (indeed, limited only by friction, vibrations and drag) than what can be obtained when the experimental platform is solidly connected to the aircraft.

Because an object free-floating in the aircraft could exceed its travel limit in a very short period of time which depends on the aircraft acceleration history and the release conditions, a number of experiments have been performed on a one-dimensional (z-axis) LMIM in the KC-135 to determine the time of free-fall before the limit of travel is exceeded [1, 2, 3]. The system has also been modelled to give statistical results with reasonable accuracy. From the instant of release at the start of the zero-g parabola, a 5 second free-float period can be obtained for approximately 50% of the attempts. The range of free-float times is from 1 second to 13 seconds. With optimum release conditions the free-float period can be extended to about 8 seconds with 50% assurance.

Motion isolation reduced accelerations transmitted from the aircraft to the object to under 5 mg during the free-fall period and much of that value was due to instrumentation noise.
Active gravity cancellation has also been proposed and can be achieved by using linear motors to actuate one or several degrees of freedom [3].

In this paper, it is proposed that the platform carrying the zero-gravity experiment be completely isolated from the aircraft frame, by making use of active magnetic levitation. The approach is similar to the one proposed in [4, 5] for the design and control of a magnetically levitated (maglev) robot wrist for fine compliant motion. Although active magnetic levitation of the experiment platform would reduce high frequency disturbances due to aircraft frame vibrations, it would provide too little motion range to allow for the larger, low frequency deviations from free-fall due to aircraft trajectory errors. Therefore, this paper proposes a coarse-fine residual gravity cancellation system using magnetic levitation for small, high frequency motion isolation, combined with a coarse positioning system for low frequency motion isolation.
Coarse-fine motion systems have been proposed, analyzed and used before for increasing speed and dexterity in manufacturing tasks [6, 7, 8, 5]. In [5], a coarse-fine redundant manipulator using a maglev wrist was proposed. The work presented in this paper differs from what was previously reported in several ways. First, the specific problem of active zero-g control through acceleration feedback is considered and analyzed. Second, 6 DOF coarse-fine motion coordination schemes are proposed, analysed and simulated with realistic assumptions on the performance of the coarse and fine motion stages. Finally, 6 DOF tracking of a levitated platform by a coarse-motion stage is experimentally demonstrated for the first time.

This paper is organized as follows: In Section II, the new coarse-fine vibration isolation system for micro-gravity experiments is proposed and some overall design ideas are presented. In Section III, the coarse-fine motion system is modelled. Control and coordination algorithms are also proposed and analysed. These involve acceleration feedback and the use of coarse and fine sensors for tracking of the free-falling experiment platform. In Section IV, motion simulation results are presented under realistic design assumptions and using measured acceleration data from NASA KC-135 parabolic flights. In Section V, the experimental setup used to demonstrate the feasibility of the proposed system is described and the experiments performed to date are summarized. Both simulations and experiments demonstrate that a coarse-fine motion isolation system with magnetic levitation is feasible.

II. Coarse-Fine Isolation Mount Design

There are several possible approaches to isolating the experiment platform from the aircraft carrying it. The simplest solution is just to allow the platform to float inside the aircraft, while tracking it with a coarse motion stage and latching it at the end of the free-fall parabola or whenever necessary. However, there are several good reasons to consider an active vibration isolation system. These include the ability to cancel disturbances on the experiment platform, such as pulling forces by data collection and power wires, inadvertent touching of the experiment by an operator or motion caused by reaction forces due to the experiment itself. Also, as shown

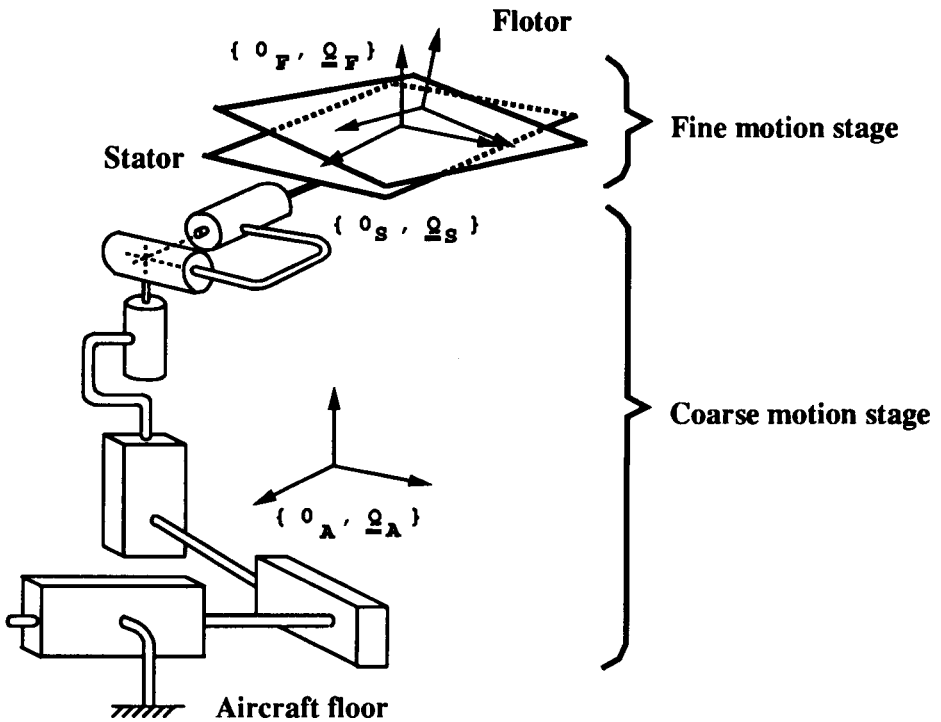

Figure 1: Overview of the proposed coarse-fine vibration isolation system.

in [1, 2, 3], the duration of free-fall of a package inside an aircraft executing a parabolic flight is strongly dependent on how it is released. An active isolation system would allow a controlled zero acceleration release at a desired instant and at a specific location in the airplane. Finally, an active large motion isolation system would allow the exertion of small centering forces on the experiment platform, in effect trading acceleration levels for experiment duration. This ability would gain in importance if the aircraft acceleration levels on parabolic flights could be decreased through better sensing and control.

Active vibration isolation solutions that involve direct mechanical linkages and that would also allow some controlled exertion of forces would be difficult to design and implement, simply because the actuator exerting the force would also transmit unwanted vibrations. Thus some active levitation method is desirable because it would allow low cutoff frequency low-pass filtering of the actuation forces. Such active levitation methods could involve magnetic-bearing type of actuators with iron in the magnetic gap or voice-coil type of actuators (or Lorentz actuators) with conductors in the magnetic gap, the latter having several advantages, some of which are the need for just a single actuator for bi-directional motion along each degree of freedom, the linearity of applied force with command current, the better force characteristic with large magnetic gaps and the simplicity of design.

The vibration isolation system proposed in this paper would use large-gap voice-coil actuators. The system overview is given in Figure 1 . The concept follows closely [4, 5]. A coarse motion stage, attached to the aircraft body, can impart fast, controlled, 3-DOF (or more) motion to the *stator* of a levitator. For simplicity, the coarse-motion stage shown in Figure 1 is a cartesian

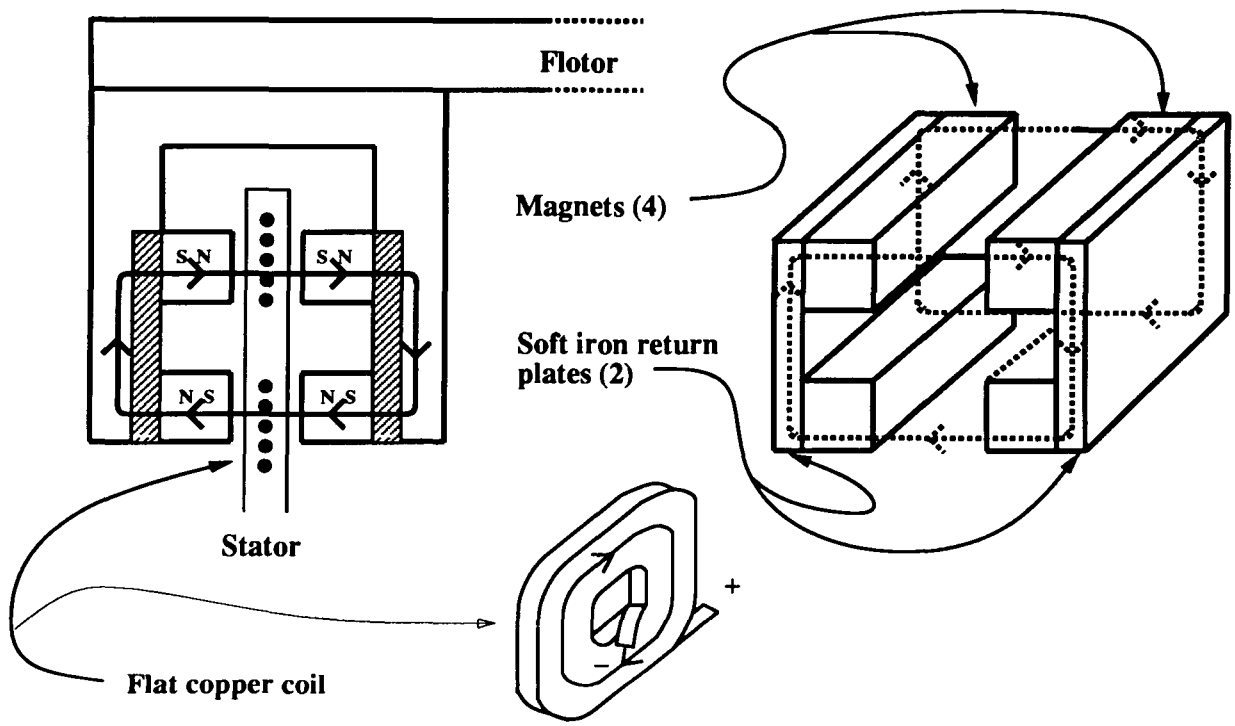

Figure 2: The schematic of the magnetic actuator used for the levitator.

robot of the gantry type equipped with a spherical wrist, but there is considerable freedom in choosing its structure.
In keeping with the terminology proposed in [5], the levitated experiment platform will be referred to as the *flotor*. The levitator's flotor is actuated by at least six moving coil or "voice coil" actuators, shown in Figure 2.

Each actuator has a magnetic assembly, attached to the flotor and a matching coil, attached to the stator. Each coil fits within the gap of the magnetic circuit created by its matching magnetic assembly, allowing only a limited motion range or *workspace* (of the order of $\pm 20 - 30$mm) of the flotor with respect to the flotor. Although the flotor is not physically attached to the stator (except, perhaps, for wires carrying signals and power) controlled Lorentz forces can be imparted to the platform by controlling the currents through the coils attached to the stator. Six linearly independent wrench vectors (6-vectors with three force and three torque components) can be generated with almost any location and orientation of the actuators. Indeed, with a suitably chosen geometry, 6 DOF motion along six degrees of freedom can be achieved without excessive coil currents [5].
With the best of current technology, it would be very difficult, if not impossible, for the levitator's voice coil motors to produce enough force to support the entire weight of the flotor under normal gravity conditions. Thus, a latch mechanism is necessary to fix the flotor under normal (or higher than normal) gravitational accelerations.

The position and orientation of the flotor with respect to the stator can be obtained by an optical sensor similar to the ones presented in [9, 4, 5] and others. An example is given in Figure 3.

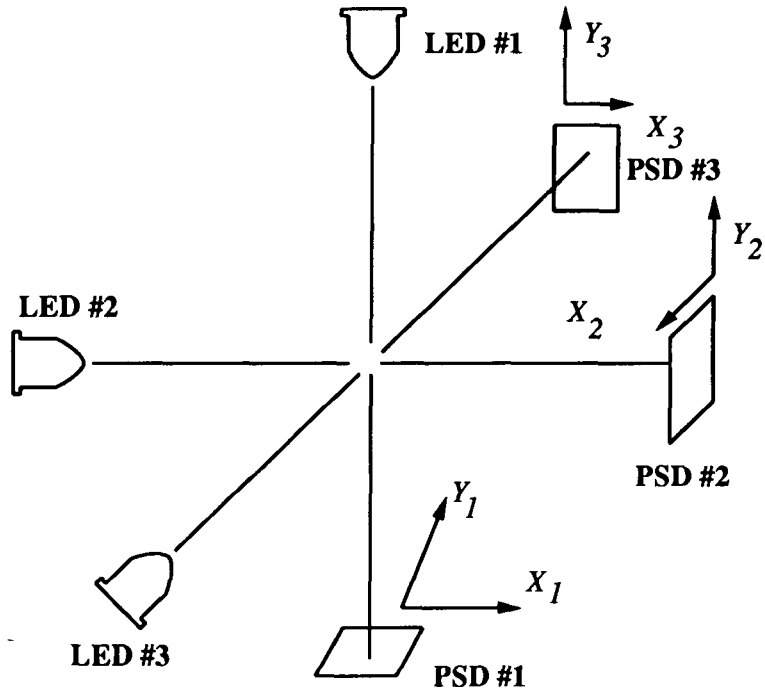

Figure 3: Optical sensing system for the levitator.

Three narrow beam light-emitting diodes are attached to the platform. They project intersecting, orthogonal beams of light on the surfaces of three orthogonal, two-dimensional, lateral-effect position sensing diodes (PSDs) [10] attached to the stator. A simple kinematic calculation (intersection of three spheres) can be used to generate the position and orientation of the flotor with respect to the stator by using the three sets of two-dimensional light spot coordinates sensed by the PSDs. The position sensing system described in Figure 3 has a limited range of motion that can be enlarged by using commercially available PSD cameras.

The performance of the coarse-fine isolation system will depend on the flight characteristics of the KC-135 aircraft. The aircraft translational acceleration levels axes are primarily stochastic during the free-fall part of the flight parabola which lasts somewhat less than 20 seconds. Typical acceleration levels are presented in [11], where it is shown that acceleration peaks perpendicular to the aircraft floor can exceed 50 mg for brief instants and can have an RMS value of 20 mg. Acceleration in the plane of the aircraft floor have much lower peak amplitudes. Thus, the coarse tracker will be expected to generate accelerations of up to 50 mg to follow the flotor in free-fall. The distance which the coarse tracker must travel is limited by the internal space in the KC-135 aircraft and is typically less than 1.5 m in the vertical direction when allowance is made for a real experimental package and installation facilities.

III. Modelling and Control

The following coordinate systems are defined and shown in Figure 4:

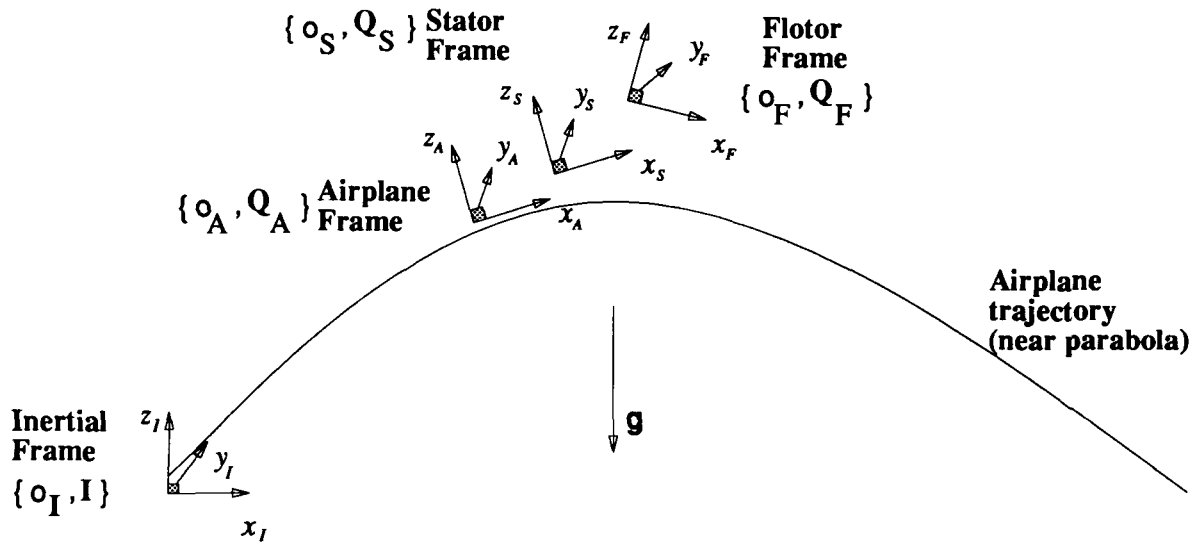

Figure 4: The coordinate systems describing the motion isolation system.

- $\{o_A, \mathbf{Q}_A\}$, attached to the aircraft frame at the nominal center of the coarse motion stage workspace.
- $\{o_S, \mathbf{Q}_S\}$, attached to the levitator's stator.
- $\{o_F, \mathbf{Q}_F\}$, attached to the flotor's center of mass and aligned about its principal axes of symmetry. When the flotor is in its nominal position, the flotor and stator coordinate systems coincide.
- an inertial system $\{o_I, \mathbf{I}\}$, whose origin coincides with with o_A at the start of the free-fall parabola. The identity matrix $\mathbf{I}$ is chosen as illustrated in Figure 4, with the z-axis being aligned with the gravitational force, and the initial aircraft velocity lying in the yz-plane. ($\mathbf{g} = [00 - 9.81]^T$).

All vectors and matrices expressed in the inertial system will be shown in bold letters.
We assume that the flotor (and the experimental platform it carries) can be accurately modelled by a rigid body having mass m and inertia matrix $\mathbf{J}$ *with respect to its center of mass* in the inertial coordinate system. In flotor coordinates, the flotor's inertia matrix becomes $J = \mathbf{Q}_F{}^T \mathbf{J} \mathbf{Q}_F$. Let $\mathbf{a}$ and $a = \mathbf{Q}_F^T \mathbf{a}$, $\boldsymbol{\omega}$ and $\omega = \mathbf{Q}_F^T \boldsymbol{\omega}$ denote the flotor's acceleration and angular velocity in inertial and, respectively, flotor coordinates, let $\mathbf{f}$ denote the force acting on the flotor, and let $\boldsymbol{\tau}$ denote the torque acting at the flotor's center of mass.
It is well known that the flotor's rotational motion is described by the following differential equations:

$$\frac{d}{dt}\mathbf{Q}_F = \boldsymbol{\omega} \times \mathbf{Q}_F \quad ; \quad \frac{d}{dt}(\mathbf{J}\boldsymbol{\omega}) = \boldsymbol{\tau} \tag{1}$$

where, for any vector $\mathbf{v} = [v_1 \ v_2 \ v_3]^T$

$$\mathbf{v}\times = \begin{bmatrix} 0 & -v_3 & v_2 \\ -v_3 & 0 & -v_1 \\ -v_2 & v_1 & 0 \end{bmatrix} \quad . \tag{2}$$

In flotor frame, the equations of motion of the flotor are simply Newton's law and Euler's equation:

$$ma = mg + f + f_d \quad ; \quad J\dot{\omega} + \omega \times J\omega = \tau + \tau_d \quad , \tag{3}$$

where $\boldsymbol{\omega} = \mathbf{Q}_F\omega$, $\mathbf{f} = \mathbf{Q}_F f$, $\mathbf{g} = \mathbf{Q}_F g$, $\boldsymbol{\tau} = \mathbf{Q}_F\tau$, and $\mathbf{f}_d = \mathbf{Q}_F f_d$ and $\boldsymbol{\tau} = \mathbf{Q}_F\tau_d$ are disturbance forces and torques (from eddy-current coupling between flotor and stator, flow of air, dragging power wires, etc).

The coarse-motion stage should have at least three, but preferably six, degrees of freedom. It is assumed that the coarse-motion has a closed-loop controller that servoes the stator's position and orientation with respect to the aircraft frame, *i.e.*, that the coordinates ${}^A r_{AS}$ of $o_S - o_A$ in $\mathbf{Q}_A$ frame ($o_S - o_A = \mathbf{Q}_A {}^A r_{AS}$) and ${\mathbf{Q}_S}^{-1}\mathbf{Q}_A = {\mathbf{Q}_S}^T\mathbf{Q}_A$ are available and controllable. A reasonable assumption on the behaviour of the the stator position under feedback control is that of a second order system with limits on velocity and acceleration:

$${}^A\ddot{r}_{AS} + 2\zeta\omega_0 {}^A\dot{r}_{AS} + {\omega_0}^2 {}^A r_{AS} = {\omega_0}^2 {}^A r_{AS_d} \tag{4}$$

$$\| {}^A\ddot{r}_{AS} \| < a_{max} \tag{5}$$

$$\| {}^A\dot{r}_{AS} \| < v_{max} \tag{6}$$

where ω_0 determines the cutoff frequency at which the stator can no longer track the command input ${}^A r_{AS_d}$ and the damping coefficient ζ determines the overshoot of the response. In the above equations, the characteristic frequency, damping ratio and acceleration and velocity bounds are the same for each axis, but these can be selected to match a particular coarse-motion stage, once it will be selected. In case the coarse-motion stage has more than 3 DOF, similar assumptions can be made on the stator orientation servo by using some appropriate orientation parametrization.

It will be assumed that the disturbance forces exerted on the stator in reaction to forces applied by the levitator, as well as the effects of the aircraft motion, have negligible effects on the coarse-stage motion. If this is not the case, a detailed stability analysis of the coupled motion of the coarse and fine systems should be done along the lines of the work presented in [8]. During the free-fall part of the flight, the acceleration levels do not exceed 50 mg [11], so even with a heavy experiment platform (300 lb or so), the forces required to completely stop the platform motion are quite small.

Because of the limited motion range of the flotor with respect to the stator, the flotor will quickly exceed its motion range, even with small deviations of the aircraft trajectory from an ideal parabola. Therefore, during the free-fall part of the aircraft flight, the commanded stator position should coincide with the flotor position, *i.e.*, ${}^A r_{AS_d} = {}^A r_{AF}$, where $o_F - o_A = \mathbf{Q}_A {}^A r_{AF}$. The

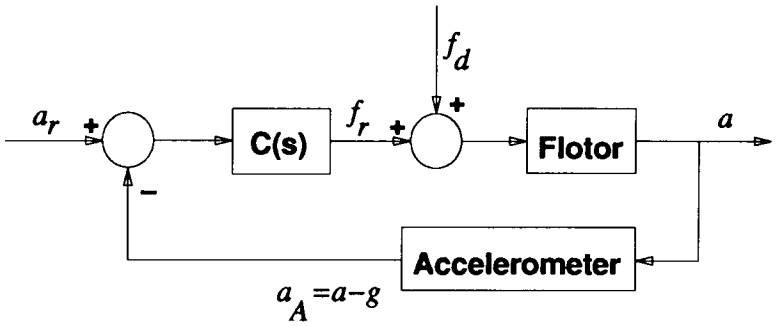

Figure 5: Control loop for the flotor acceleration feedback.

coordinates ${}^{A}r_{AF}$ can be obtained from the combined measurement of the stator with respect to the aircraft (through the conventional sensors of the coarse-motion stage) and that of the flotor with respect to the stator (through the levitator's optical sensor).

III.a. Flotor Acceleration Feedback

It will be assumed that accelerometers are used to measure the acceleration **a** of o_F with respect to an inertial frame. Since accelerometers are attached to the flotor, the flotor frame coordinates a of the flotor acceleration are available.
Once the flotor can be released, the resultant f of its actuators' action is some compensated function of the acceleration error, as shown in Figure 5. In terms of Laplace transforms,

$$\hat{f}(s) = \hat{c}(s)(\hat{a}_r(s) - \hat{a}(s)). \tag{7}$$

where $\hat{c}(s)$, $\hat{a}(s)$ and $\hat{a}_r(s)$ are the Laplace transforms of the feedback compensator, the flotor acceleration and the required acceleration, respectively. Due to the simplicity of the flotor dynamics (single rigid mass) in Figure 5, *any* proper, stable, real-rational transfer function can be obtained from the desired acceleration a_r to the actual acceleration a of the flotor (of course, there will be limits on achievable performance due to plant uncertainty, actuator saturation, etc.). Choosing a first order stable transfer function leads to a compensator $\hat{c}(s)$ that is simply an integrator, *i.e. velocity* feedback:

$$\hat{f}(s) = k\frac{1}{s}(\hat{a}_r(s) - \hat{a}(s)), \tag{8}$$

which leads to

$$\hat{a}(s) = \frac{\frac{k}{m}}{s + \frac{k}{m}}\hat{a}_r(s) + \frac{s}{s + \frac{k}{m}}g + \frac{\frac{1}{m}s}{s + \frac{k}{m}}\hat{f}_d(s). \tag{9}$$

Usually, a is measured by a proof-mass accelerometer providing a signal $a_A = a - g$ (thus zero in free fall). In terms of this signal, the above equation becomes

$$\hat{a}_A(s) = \frac{\frac{k}{m}}{s + \frac{k}{m}}[\hat{a}_r(s) - g] + \frac{\frac{1}{m}s}{s + \frac{k}{m}}\hat{f}_d(s). \tag{10}$$

Clearly, for reasonably high gain k, the acceleration of the flotor and platform *does indeed track the desired acceleration* a_r and *rejects the disturbance force* f_d. Usually, $a_r = g$, leading to $\hat{a}_A(s) \to 0$, although, as it will be seen later, this may not always be the best approach.
The angular acceleration of the flotor can be controlled in a similar way, , *i.e.*, by using angular velocity feedback. The flotor angular acceleration can be regulated to zero by the control law $\tau = -k_\omega J\omega$, with some positive gain k_ω. Indeed, consider the Lyapunov function $V = \frac{1}{2}\omega^T J\omega$. Along the trajectories described by the Euler equation in (3) (with $\tau_d = 0$), we have that

$$\dot{V} = \frac{1}{2}[\omega^T(\tau - \omega \times J\omega) + (\tau - \omega \times J\omega)^T\omega] = \omega^T\tau = -k_\omega\omega^T J\omega < 0. \tag{11}$$

Thus the signal $\delta = -\omega \times J\omega$ is bounded and decreases to zero. By taking the Laplace transform of Euler's equation and letting $a_\omega = \dot{\omega}$, we obtain that

$$\hat{a}_\omega(s) = \frac{s}{s + k_\omega} J^{-1}\hat{\delta}(s), \tag{12}$$

so the angular acceleration of the flotor should be kept small at low frequencies.

Before moving on, a comment on the nature of the disturbances acting on the flotor (or experimental platform) and on means of rejecting them is in order. On one hand, disturbance forces can be both unknown and very difficult to measure, *e.g.* forces due to an experiment operator touching the flotor. The only hope of attenuating these disturbances is through accelerometer feedback. On the other hand, some unpredictable disturbances can be easily measured, *e.g.* the forces and torques applied to the flotor by an umbilical carrying signals and power. These disturbances can be rejected to a large extent through *feed-forward through the flotor's actuating coils*, while accelerometer feedback is still in effect.
Umbilical disturbances can be measured by means of standard strain-gauge force-torque sensors or through other, more sophisticated, techniques. Even magnetic levitation can be used, with the same proof-mass principle used in some accelerometers. For example, the umbilical can be attached to the flotor through an intermediate levitated proof-mass (*i.e.*, another flotor), whose position and orientation is servoed to that of the experimental platform. By monitoring the forces needed to keep the proof-mass in place (*e.g.*, by monitoring the coil currents of Lorentz actuators, if the proof-mass uses Lorentz levitation), one obtains the forces and torques exerted by the umbilical.

III.b. Acceleration Feedback with Centering Motion

Although, ideally, the desired flotor acceleration a_r is zero, in practice, even the coarse motion platform will "run out of space" because of errors in the aircraft trajectory. Instead of letting the platform reach its motion limit (with associated high acceleration due to hard mechanical contact), it may be instead desirable to provide low-level "drift" accelerations that tend to bring the flotor to the nominal center of the coarse motion platform. We will assume that this nominal center coincides with the aircraft reference frame origin o_A. There are a couple of ways in which a centering drift motion can be obtained. First, one can modify the control action (8) by

adding a proportional derivative term in the flotor offset $r_{FA} = \mathbf{Q}_F{}^T(o_A - o_F)$ with respect to the aircraft frame:

$$\hat{f}(s) = k\frac{1}{s}[\hat{a}_r(s) - \hat{a}(s)] + k_p\hat{r}_{FA} + k_v s\hat{r}_{FA}, \tag{13}$$

where k_p and k_v are positive and small. The coordinates r_{FA} of $o_A - o_F$ in flotor frame are obtained from the coarse-stage and levitator's sensors.
With $k = 0$ in the above (to see what the effect of this centering force is), applying this PD controller to Newton's equation in (3) (expressed in inertial coordinates) leads to

$$m\frac{d^2}{dt^2}(o_F - o_I) = m\mathbf{g} + \mathbf{Q}_F(k_p r_{FA} + k_v\dot{r}_{FA}) + \mathbf{f}_d. \tag{14}$$

Therefore, in inertial coordinates, the equation of motion of the flotor coordinate system origin with respect to the aircraft frame becomes

$$\frac{d^2}{dt^2}(o_F - o_A) + \frac{k_v}{m}\frac{d}{dt}(o_F - o_A) + \frac{k_p}{m}(o_F - o_A) = \frac{k_v}{m}\boldsymbol{\omega} \times (o_F - o_A) + \frac{1}{m}\mathbf{f}_d, \tag{15}$$

where we made use of the fact that

$$\frac{d}{dt}(o_F - o_A) = \boldsymbol{\omega} \times \mathbf{Q}_F r_{FA} + \mathbf{Q}_F\dot{r}_{FA} = \boldsymbol{\omega} \times (o_F - o_A) + \mathbf{Q}_F\dot{r}_{FA} \tag{16}$$

and

$$\frac{d^2}{dt^2}(o_A - o_I) = \mathbf{g} \tag{17}$$

(note that errors in aircraft trajectories are included in $\mathbf{f}_d$).
The angular acceleration $\boldsymbol{\omega}$ of the levitator's flotor should be small, even without angular acceleration servoing, because the aircraft rotates relatively slowly during the parabolic flight. Therefore, the error $o_F - o_A$ of equation (15) should be small. In addition, due to the orthogonality of $\boldsymbol{\omega} \times (o_A - o_F)$ to the centering force $\frac{k_p}{m}(o_F - o_A)$ acting on the flotor, it should be possible to use a Lyapunov argument to show that, in the absence of disturbance forces $\mathbf{f}_d$ and assuming that $\boldsymbol{\omega}$ is bounded, $o_F - o_A$ converges to zero.
Therefore, by using *only local* information (*i.e.*, no inertial reference) the flotor can be made to track the aircraft center. Note that, in order to insure low accelerations, the constants k_p and k_v should be made as small as possible.

As a second way to achieve a centering force on the flotor, note that the desired acceleration a_r of (8) can be set according to a PD law similar to (13), *i.e.*,

$$\hat{a}_r(s) = k_p r_{FA} + k_v s r_{FA}. \tag{18}$$

If the acceleration controller works well, a should track $a_r - g$ closely (see equation (10)), so, in effect, (13) will be quite well approximated. Of course, for such an approach to work, the

acceleration gain of (8) should lead to a substantially faster time constant than the time constants associated with (18).
It is also possible to make the gains k_p and k_v depend on how close the platform is to the aircraft walls - the larger $o_F - o_A$, the larger k_p and k_v. In particular, a moderately large workspace without drift can be implemented by setting these gains to zero within a certain radius $||o_F - o_A|| < r$.

A corrective term for drift in the orientation of the platform can also be devised. In particular, if the coarse-motion stage is only a 3-DOF system, as the airplane goes through a parabola, the levitator's stator will change orientation with it. Therefore, in spite of being free to move in translation, *the flotor orientation must track that of the stator.* Tracking could be achieved by using a control scheme based on the vector part of the Euler quaternion, as done in [5]. The rotation matrix $Q_{AF} = \mathbf{Q}_A{}^T\mathbf{Q}_F$ of the flotor with respect to the aircraft is represented by the Euler quaternion $[\beta_0\,\beta^T]^T$ as

$$Q_{AF} = \exp(\phi\,\mathbf{s}\times) = I + 2\beta_0\,\beta\times + 2(\beta\times)^2 \quad , \tag{19}$$

where $\mathbf{p} = [\beta_0\,\beta^T]^T = [cos(\phi/2)\,sin(\phi/2)s^T]^T$, and s and ϕ are the normalized axis ($\|s\| = 1$) and, respectively, the angle of the rotation matrix Q_{AF}. This parametrization has several advantages, the most important one being the explicit representation of the axis of rotation.
It can be shown [12] that after linearization (approximate or by exact cancellation of the dynamics, as in computed torque control), for rotation angles less than 180 degrees, the flotor's rotational dynamics is given by

$$\ddot{\beta} \;=\; \frac{1}{2}J^{-1}\tau \tag{20}$$

Similarly to (13), a PD term can be added to the flotor torque in such a way as to bring the orientation of the flotor towards some central orientation aligned with the aircraft:

$$\tau = -\tilde{k}_p\beta - \tilde{k}_v\dot{\beta} \quad , \tag{21}$$

where the orientation vector β that corresponds to $\beta_0 \geq 0$ can be obtained from (19) and is given by

$$\beta\times = \frac{1}{2(1 + \mathrm{tr}Q_{AF})^{\frac{1}{2}}}(Q_{AF} - Q_{AF}{}^T), \tag{22}$$

where $\mathrm{tr}Q_{AF}$ denotes the trace of Q_{AF}.

It is clear that, when the platform acceleration is not measured, there can be no acceleration error correction for the platform. This is probably no serious drawback, because the platform is in near free-fall condition (except for some interaction with the coarse motion stage through eddy current damping and very little air drag). The coarse-motion stage can still be used to track the platform and the moving coil actuators can still be used to center the flotor. However, some of the control over the acceleration levels exercised on the flotor is lost.

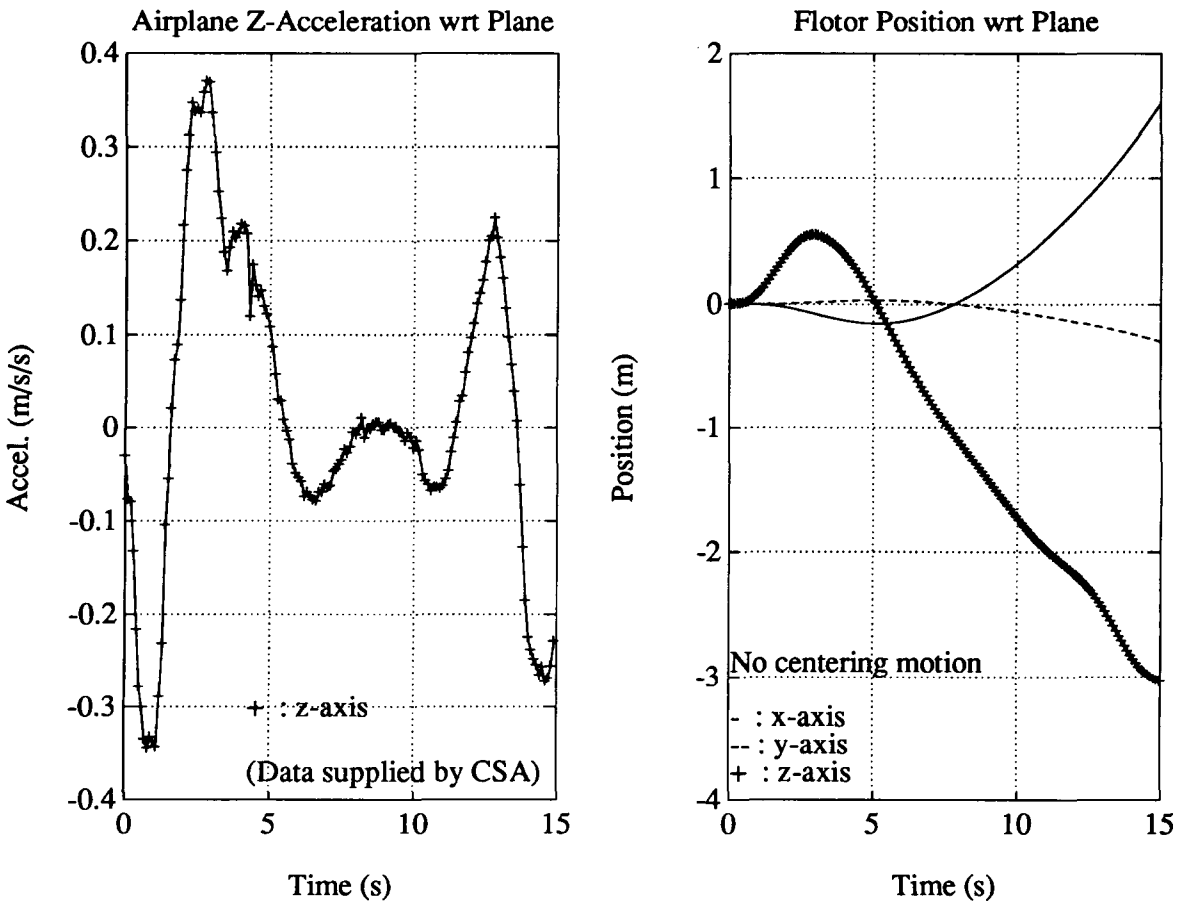

Figure 6: The position of the platform with respect to the airplane with a given disturbance in the z-axis of the airplane.

IV. Simulation Setup and Results

The motion of the system described in Section I, with the control laws described in Section II, was simulated using the software packages PRO-MATLAB^{TM} and SIMULAB^{TM}, by The MathWorks. The complete simulation was performed by describing the equations of motion of every component of the system *i.e.*, the flotor dynamics, the stator dynamics, and the aircraft kinematics, in the inertial coordinate system $\{o_I, \mathbf{I}\}$. The control algorithms presented in Section II were applied in local coordinates as described, *i.e.*, the flotor control algorithms were expressed in flotor coordinates, the coarse-motion stage dynamics were expressed in aircraft coordinates and the aircraft kinematics were expressed in inertial coordinates.

Acceleration data obtained on NASA KC-135 parabolic flights [11] were used to drive the aircraft kinematics. Although there was no measured data available on the orientation of the KC-135 during flight, the initial aircraft orientation at the start of the parabola and the final orientation at the end of free-fall are fairly well known. These show that the aircraft undergoes a change in pitch angle of about -60 degrees and is rolling to the right roughly 20 degrees during the free-fall

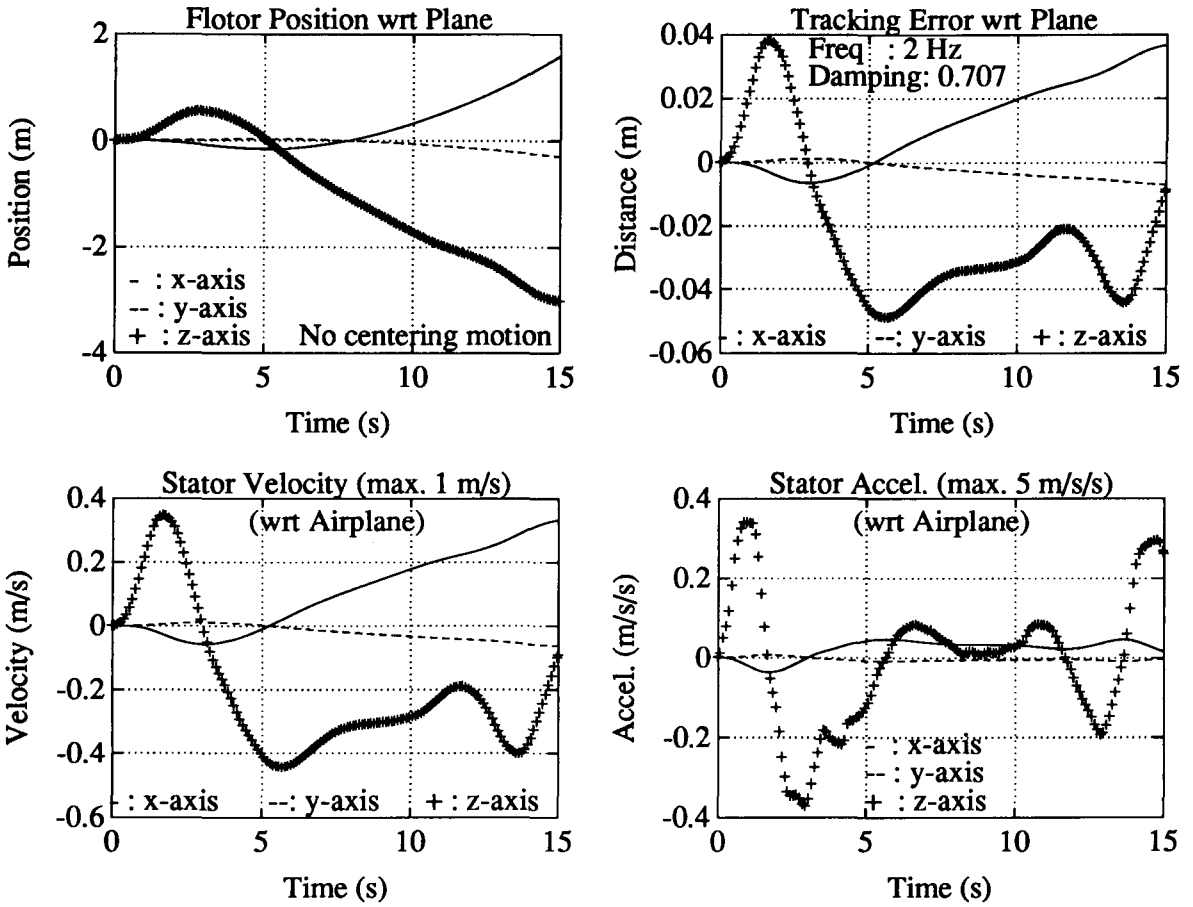

Figure 7: Flotor-stator tracking errors and stator velocity and acceleration.

parabola. In all the simulations performed, it was assumed that this rotation occurs at a constant angular rate, about the fixed Euler eigenaxis of rotation between the initial and final orientations.

Some typical results are displayed in Figures 6, 7, 8 and 9. Unless otherwise specified, airplane coordinates are used.

Figure 6 shows the acceleration data and the flotor position. Figure 7 shows the tracking errors in x, y, z. As expected, the coarse-motion stage tracking error along the z-axis is substantially larger than for the x and y axis. With fairly stringent performance limitations on the coarse motion stage (2 Hz bandwidth, 5 m/s/s max. acceleration, 1 m/s max. velocity), typical tracking errors are about ± 10 mm in the y-axis, ± 30 mm in the x-axis and ± 40 mm in the z axis. These errors are reduced drastically as the bandwidth of the tracking platform is increased. It is fairly simple to design a wide-gap levitator that matches these workspace requirements. For example, the stator could be shaped as a rectangular shell with flat coils (as shown in Figure 2) embedded in its walls. The matching flotor would have a large face available for an experiment platform, and would have a substantial travel in the z axis, while maintaining relatively small magnetic gaps for the actuators. The optical sensor shown in Figure 3 could be employed with minor

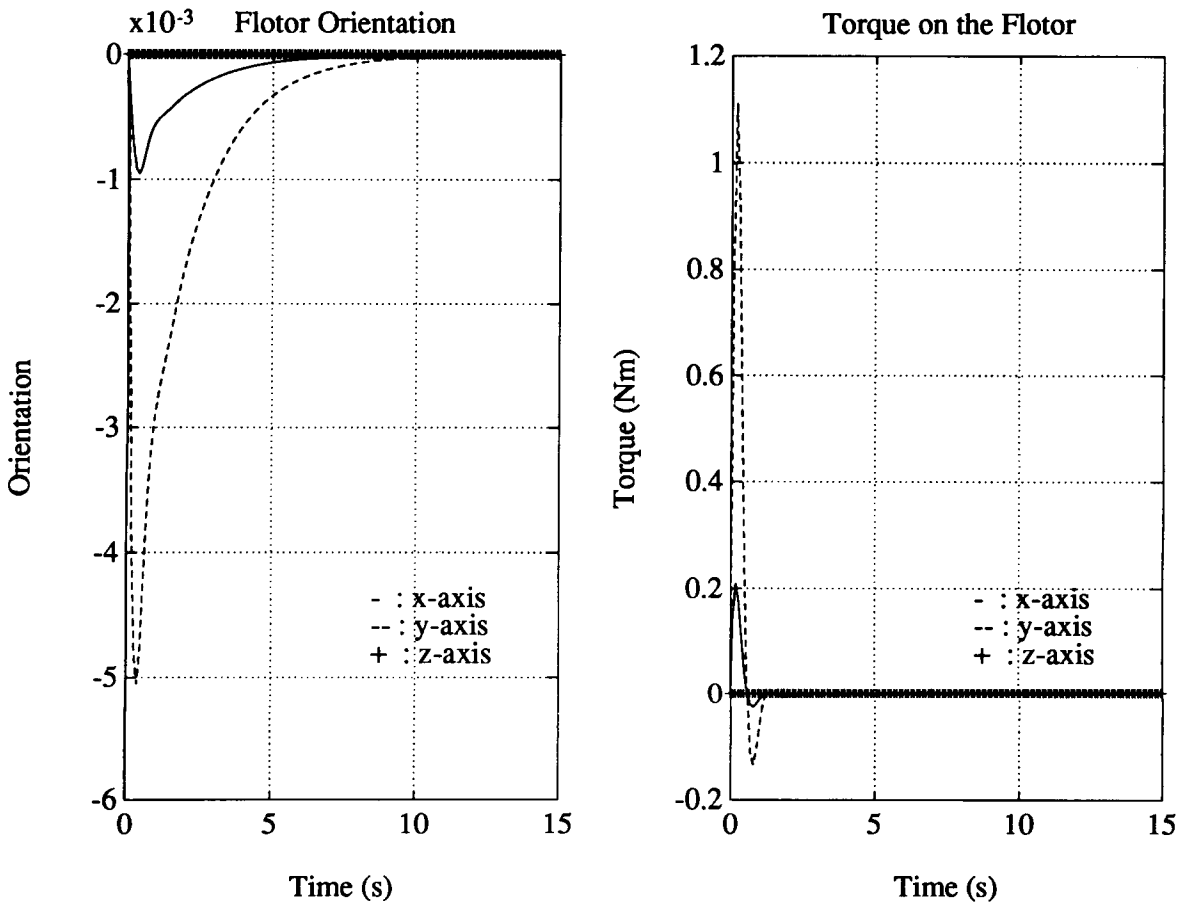

Figure 8: Orientation error components and torque applied to the flotor.

modifications for the large z-axis travel.

Figure 8 shows the rotation tracking performance (the vector part β of the Euler quaternion, as defined for equation (19), is displayed) and the torques applied to the flotor. It can be seen that the orientation errors are small and that the torques required to rotate the flotor are small (the flotor is modelled as a 300 lb cube).

Figure 9 shows the trade-off between acceleration quality and free-fall duration. Simulation results with two sets of centering gains in equation (18) are displayed. It can be seen that as these gains are increased, the flotor moves less with respect to the aircraft. At the same time, the acceleration levels on the flotor increase, as expected. If the required acceleration level for a given experiment is known, one can modify the centering acceleration of equation (18) in order to optimize experiment duration. Another possible use for centering forces is the avoidance of "crashes" into the aircraft walls.

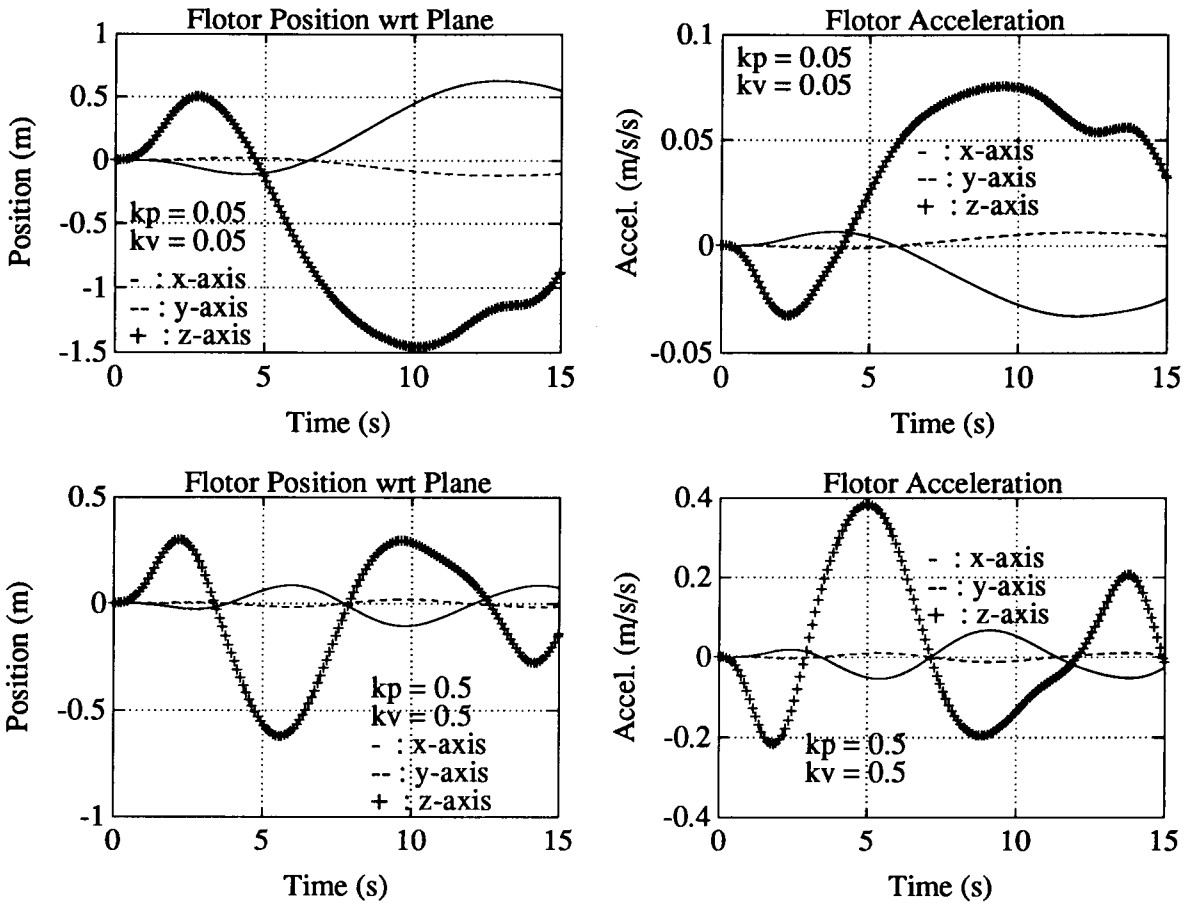

Figure 9: Effects of centering control on position and acceleration.

V. Experimental Setup and Results

To demonstrate the feasibility of the coarse-fine motion isolation system described in Section I and the validity of the control and coarse-fine motion coordination schemes presented in Section II, the authors used a Unimation PUMA 500 robot equipped with a magnetically levitated fine-motion robot wrist, developed and built in the Electrical Engineering Department at UBC. The UBC maglev wrist uses the same design principles applied to the "Magic" wrist described in [4, 5] and outlined in Section I of this paper. The weight of its flotor is 0.640 kilograms, its motion range is ± 4.5 mm and ± 7 degrees from the nominal center. Each of the wrist's voice-coil actuators produces roughly 2 N/A force per unit current and the power consumption required to "fly" the flotor without any additional payload is less than 7 Watts.

The real-time system employed for the coordinated control of the PUMA robot and the levitator's flotor is illustrated in Figure 10. An IBM PC-AT compatible computer hosts a Spectrum Inc. digital signal processing (DSP) board using a Texas Instruments Inc. TMSC30 DSP chip, as well as analog input and output boards linked through a fast, private bus. The PC

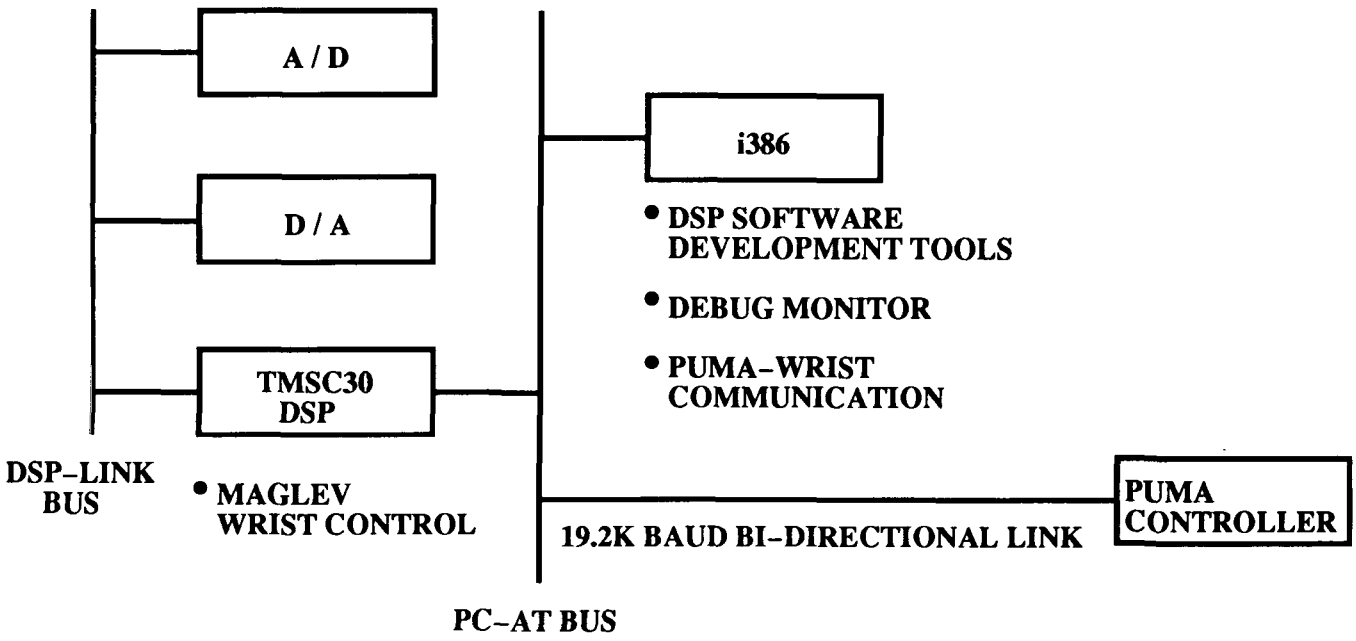

Figure 10: The block diagram of the PUMA-Wrist real-time controller.

is connected through a 19.2 Kbaud serial link to the PUMA robot controller.

The floating point DSP board controls the levitator's flotor, computes the stator's position and orientation from position and Euler angles information obtained from the robot through the serial link, and calculates the updated robot set points (δx, δy, δz, roll, pitch, yaw) as a function of flotor position. The kinematic calculations required to determine the flotor position with respect to the stator are exactly as described in [5]. The flotor controls are updated every 1.5 milliseconds, with the DSP board running at about 1 Mflop.
The PC is used for DSP software development and for the serial port communications between the wrist controller and the robot controller.
A program written in VAL II handles the serial communications on the PUMA controller side, while the robot is in INTERNAL ALTER mode, effectively making it a slave to the wrist's flotor motion. The coordination data between the robot and the wrist could only be transmitted every 56 milliseconds. This could be improved substantially if the PUMA controller could be modified. In particular, a Jacobian-based velocity tracking algorithm that does not require the on-line solution of the inverse kinematics problem could be implemented.

Coordinated motion of the flotor and the robot was demonstrated by the authors, with the robot following the wrist's flotor position and orientation. Translational tracking with locked orientation was also demonstrated.
Accelerometers were mounted on the flotor, but problems with drift and noise have so far prevented successful implementation of acceleration feedback.

VI. Conclusion

The authors proposed a coarse-fine large-motion isolation system for residual gravity cancellation on parabolic flights. The system would use wide gap magnetic levitation for vibration isolation and acceleration servoing of an experimental platform. The proposed isolation mount was modelled and control algorithms for acceleration servoing and centering motion were presented. The model and the control algorithms were simulated and an experimental coarse-fine system using a PUMA robot and maglev wrist was put together in order to demonstrate the system's feasibility.

The proposed gravity cancellation system has several advantages, among which are (i) the ability of reducing the dynamic coupling between the aircraft and experimental platform to just eddy current coupling, (ii) the ability of using maglev forces to obtain good initial release of the experiment platform, (iii) the ability of trading off experiment duration versus quality of the free-fall.

The simulation results and experimental results presented seem to indicate that such a coarse-fine approach to vibration isolation is feasible. In particular, the ability of a coarse-motion stage to track a levitated platform was demonstrated through both simulations and experiments. The only requirement left to demonstrate that the coarse-fine motion isolation system will work as proposed is the successful application of acceleration feedback. That work is now in progress.

Acknowledgements

The authors wish to thank David Fletcher for machining the maglev wrist used in their experiments, Dr. Dale Cherchas for providing space and experimentation time in his lab, and Nelson Ho for general help and for writing the symbolic debug monitor for the DSP. The support of NSERC and the Canadian Space Agency is gratefully acknowledged.

References

[1] A. Adler and J. Bernaldez. Motion isolation mount for microgravity. Technical report, Dept. of Physics, University of British Columbia, December 1989. Engineering Physics Project No. 8918.

[2] H. Davis. Report on the proposed modifications to the 1-d large motion isolation mount for flight tests on the NASA KC-135 aircraft. Technical report, Engineering Physics, University of British Columbia, October 1990. (prepared for NRC under contract 31016-0-6022/01-SW).

[3] H. Davis. Report on the first flights of the large motion isolation mount on the NASA KC-135 Aircraft, june 5-9, 1990. Technical report, Engineering Physics, University of British Columbia, September 15 1990. (prepared for NRC under contract 31016-0-6022/01-SW).

[4] R.L. Hollis. Magnetically levitated fine motion robot wrist with programmable compliance, October 1989. U.S. Patent number 4,874,998.

[5] R.L. Hollis, S. Salcudean, and P.A. Allan. A Six Degree-of-Freedom Magnetically Levitated Variable Compliance Fine Motion Wrist: Design, Modelling and Control. *IEEE Transactions on Robotics and Automation*, 7(3):320–332, June 1991.

[6] R. H. Taylor, R. L. Hollis, and M. A. Lavin. Precise manipulation with endpoint sensing. *IBM J. Res. Develop.*, 2(4):363–376, July 1985.

[7] Andre Sharon and David Hardt. Enhancement of robot accuracy using endpoint feedback and a macro-micro manipulator system. In *American Control Conference proceedings*, pages 1836–1842, San Diego, California, June 6-8 1984.

[8] S. Salcudean and C. An. On the control of redundant coarse-fine manipulators. In *Proceedings of the IEEE International Conference on Robotics and Automation*, pages 1843–1840, Scottsdale, Arizona, May 14-18 1989.

[9] A.E. Brennemann, R.L. Hollis, and R.H. Taylor. General position and orientation sensor for fine motions and forces. *IBM Technical Disclosure Bulletin*, 26(9):4457–4462, February 1984.

[10] United Detector Technology. Silicon photodetectors catalog. 12525 Chandron Ave., Hawthorne, CA 90250.

[11] B. V. Tryggvason. Acceleration Levels on the KC-135. Technical report, Canadian Space Agency, October 1990. Report CSA-CAP.008.

[12] S. Salcudean. On the control of magnetically levitated robot wrists. In *Proceedings of the 27th IEEE Conference on Decision and Control*, pages 186–191, Austin, Texas, December 1988.